Neutrons from ^{9}Be(α,n) Reaction for E_α between 6 and 10 MeV*

Victor V. Verbinski,† Francis G. Perey, J. Kirk Dickens, and Walter R. Burrus

Oak Ridge National Laboratory, Oak Ridge, Tennessee

(Received 28 August 1967; revised manuscript received 1 February 1968)

Absolute differential cross sections have been measured as a function of angle and α bombarding energy for the reaction ^{9}Be$(\alpha,n)^{12}$C leaving ^{12}C in its ground, first excited, and second excited states. The angular distribution for the ground-state (0+ state) transition changed from a fore-aft peaking at $E_\alpha = 6.8$ MeV to a three-peaked angular distribution at $E_\alpha = 9.9$ MeV. Similar behavior was observed for the second-excited-state transition (0+). The angular distribution for the first-excited-state transition (2+) displayed fore-aft peaking and was not sensitive to bombarding energy. A strong, low-energy component, present at forward angles at all bombarding energies, can be accounted for by three- and four-body breakup reactions.

I. INTRODUCTION

ENERGY spectra of neutrons produced by ^{4}He^{++} ion bombardment of ^{9}Be were measured as a function of neutron-emission angle θ and bombarding energy E_α, for $E_\alpha = 6$ to 10 MeV. Three neutron groups, the n_0, n_1, and n_2 neutron groups from the ^{9}Be$(\alpha,n)^{12}$C reaction, leaving ^{12}C in the ground, first, and second excited states, were well resolved in these spectra. Below these groups lay a continuum of lower-energy neutrons from the very broad n_4 level and from other, lower Q value, reactions. Without a complex shape analysis[1] these low-energy neutron groups cannot be resolved, so that the low-resolution neutron spectrometer used for these measurements proved to be an adequate choice.

Angular distributions reported previously for $E_\alpha = 6$ MeV (Ref. 2) and 10 to 22 MeV (Refs. 3 and 4) indicate that, for the n_0 group, the data are insensitive to bombarding energy E_α from 10 to 22 MeV but that at $E_\alpha = 6$ MeV the angular distribution is quite different. The present measurements therefore fill the in gap for this interesting case, and for the n_1 and n_2 angular distributions as well.

The neutron spectrum above 0.5 MeV (the cutoff value for the spectrometer used) and below the n_2 group is of interest in determining the source of the abundant low-energy neutrons. These spectra have been angle-integrated to produce $\sigma(E_n)$ and the results analyzed. The $\sigma(E_n)$ for $E_n > 0.5$ MeV were then integrated over energy, and the total cross section so obtained was compared with the flat-counter measurements of Gibbons and Macklin[5] to determine the approximate spectral behavior below the 0.5-MeV cutoff of our spectrometer.

II. EXPERIMENTAL PROCEDURE

A beam of ^{4}He^{++} ions obtained from the ORNL 5-MV Van de Graaff accelerator was energy analyzed with a 90° bending magnet, collimated, and focused on a beryllium metal target deposited on a platinum backing. The target was located at the end of a long Faraday cup. The target thickness was ≈ 1 mg/cm^2, producing an energy spread of approximately 350 keV at 10-MeV bombarding energy.

The sensing element of the neutron spectrometer was a 5-cm-diam by 5-cm-high cylinder of NE-213 liquid organic scintillator.[6] It was mounted on an RCA 6810A photomultiplier tube and positioned 45 cm from the beryllium target. A linear signal was obtained at dynode 10 and a pulse-shape discrimination (PSD) signal obtained from a modified Forté type PSD circuit[7,8] which utilizes pulses from dynode 14 and anode. This circuit rejected γ-ray pulses and identified proton-recoil neutron events down to about 0.3-MeV neutron energy (equivalent electron energy $\simeq 40$ keV).

The 5-MV Van de Graaff accelerator did not have short-burst capabilities at the time of the measurements, so that time-of-flight spectroscopy was not possible. Therefore, the pulses due to neutrons were sorted in a pulse-height analyzer, and the energy spectrum was obtained by unfolding the pulse-height distribution with the FERDOR code.[8] This code utilizes a response matrix[9] obtained from Monte Carlo calculations[10] of the pulse-height spectra due to monoenergetic neutrons of a large number of energies. The calculations were carried out with measured light yields for recoil protons, recoil carbon nuclei, and α particles from neutrons on carbon.

* Research sponsored by the National Aeronautics and Space Administration, under Union Carbide Corporation's contract with the U. S. Atomic Energy Commission.

† Present address: Gulf General Atomic, San Diego, Calif.

[1] A. Nilsson and J. Kjellman, Nucl. Phys. **32**, 177 (1962).

[2] N. H. Gale and J. B. Garg, Nuovo Cimento **19**, 742 (1961).

[3] J. Kjellman and A. Nilsson, Arkiv Fysik **22**, 277 (1962).

[4] M. Kondo, T. Yamazaki, and S. Yamabe, J. Phys. Soc. Japan **18**, 22 (1963).

[5] J. H. Gibbons and R. L. Macklin, Phys. Rev. **114**, 751 (1959); **137**, B1508 (1965).

[6] Obtained from Nuclear Enterprises Ltd., Winnipeg, Canada.

[7] M. Forté, A. Konsta, and C. Maranzana, in *Proceedings of the International Conference on Nuclear Electronics, Belgrade, 1961* (International Atomic Energy Agency, Vienna, 1962), Paper NE-59; V. V. Verbinski, W. R. Burrus, R. M. Freestone, and R. Textor, in *Proceedings of the International Conference on Neutron Monitoring, Vienna, 1967* (International Atomic Energy Agency, Vienna, 1967), Paper No. SM-76/13.

[8] W. R. Burrus and V. V. Verbinski, Trans. Am. Nucl. Soc. **7**, 373 (1964); W. R. Burrus and V. V. Verbinski (unpublished). W. R. Burrus and J. D. Drischler, Oak Ridge National Laboratory Report No. ORNL-4154 (unpublished).

[9] V. V. Verbinski et al., Trans. Am. Nucl. Soc. **7**, 374 (1964).

[10] R. E. Textor and V. V. Verbinski, Oak Ridge National Laboratory Report No. ORNL-4160 (unpublished).

FIG. 1. Results of unfolding some recent, accurately measured pulse-height spectra due to monoenergetic neutrons. The agreement is good except for the wiggles. These are due to the fact that the recent measurements were made with an improved detector arrangement (see Ref. 12). This resulted in a sharper pulse-height resolution than was built into the unfolding matrix used both for the data of this figure and the data of this paper. The latter data had much poorer resolution, which makes the wiggles vanishingly small.
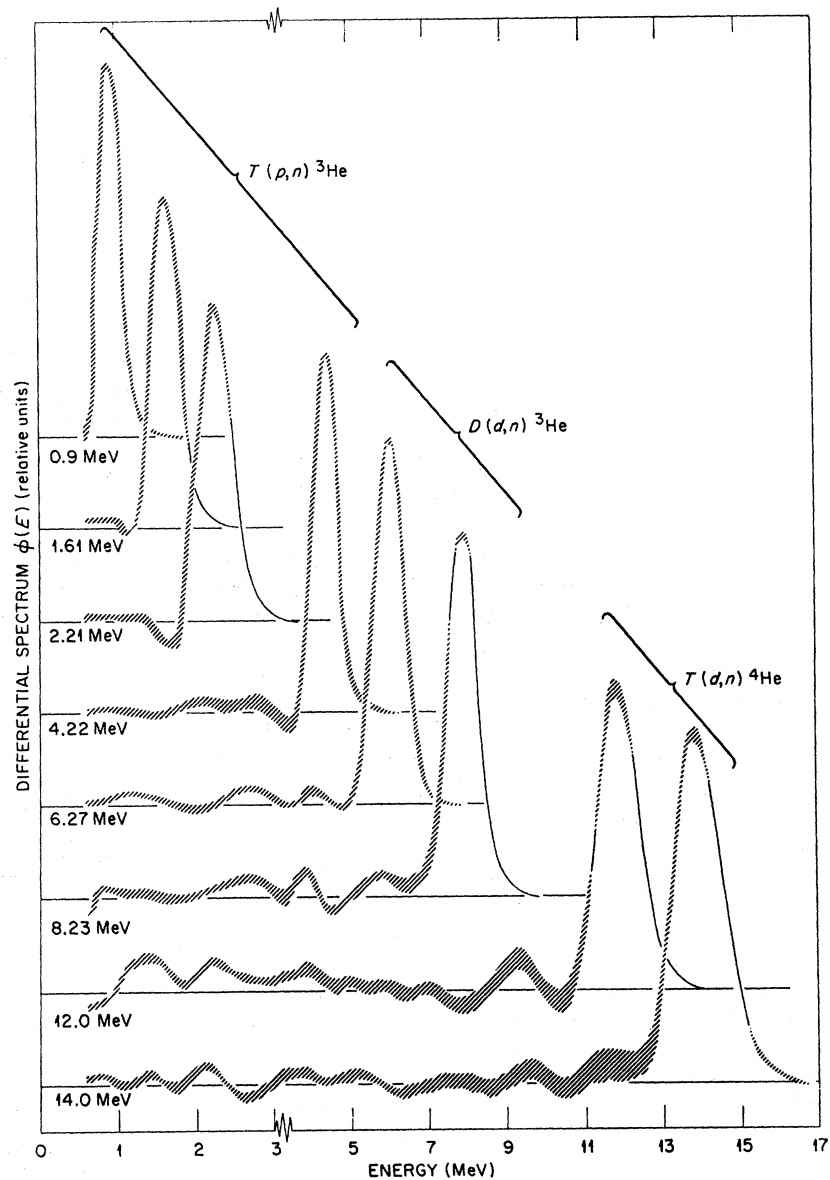
The shapes were made to match measured pulse-height distribution at the end points. They were checked with absolute experimental calibrations at 2.66- and 14.43-MeV neutron energy with the associated-particle technique.[11,12] Some recent, more accurate measurements of pulse-height spectra for monoenergetic neutrons were made[12] and unfolded with the response matrix used for the present work. The results are shown in Fig. 1. The matrix matches the new, accurate, high-resolution measurements well except for the wiggles. These are mostly due to the sharper resolution of the new measurement than is built into the matrix. With the poor resolution (n,α) measurements, the wiggles become vanishingly small.

The spectrometer was also used to obtain the integrated neutron flux from a Po–Be neutron source calibrated by the National Bureau of Standards, and agreement with the NBS value was appreciably better than 5%. The Po–Be spectrum is shown in Fig. 2, along with some careful nuclear emulsion measurements taken from the literature.[13,14]

The errors assigned to the neighboring points in the output of the FERDOR unfolding code are highly correlated. Therefore, the percentage error for the area

[11] T. A. Love, R. T. Santoro, R. W. Peelle, and N. W. Hill, Rev. Sci. Instr. 39, 541 (1968).
[12] V. V. Verbinski, W. R. Burrus, R. Textor, T. A. Love, and W. Zobel (unpublished).

[13] B. G. Whitmore and W. B. Baker, Phys. Rev. 78, 799 (1950).
[14] S. Notarrigo, R. Parisi, and A. Rubbino, Nucl. Phys. 29, 509 (1962).
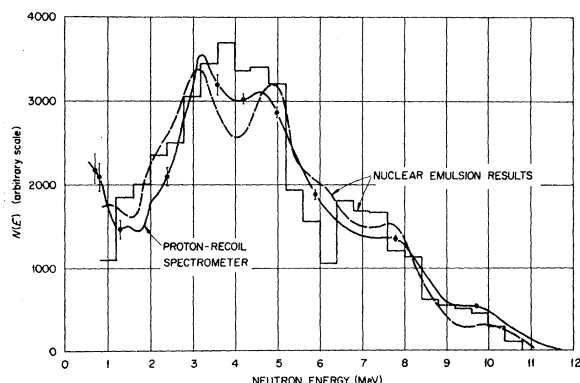
FIG. 2. Proton recoil spectrometer results for Po–Be neutron spectrum compared with nuclear-emulsion results of Ref. 13 (dashed curve) and Ref. 14 (histogram). The small ($\sim$2 cm$\times$2 cm) source, calibrated at the National Bureau of Standards, was used in determining the accuracy of the spectrometer calibration (5%).

under a peak was conservatively taken as about one-half the percentage error of the highest point. The systematic error is estimated to be 10%. Two independent evaluations of systematic error are given in Secs. III B and III E below. The sources of error include detector calibration, current-integrator calibration, Faraday-cup "leakage," and target-thickness uncertainty.

Angular distributions were measured for target and background contributions. The background was measured with a plain platinum foil as a target, and was on the order of 1%. Carbon deposition on the beryllium target and on the plain platinum blank was kept very low by using a liquid-nitrogen trap to remove diffusion-pump oil from the region of the target.

Floor scattering was ignored because only a small fraction of the source neutrons struck the floor nearby. With a 10% estimate of fast-neutron albedo from concrete, a spectrometer energy cutoff of 0.5 MeV, and an R^2 advantage of 10 for source neutrons compared with concrete albedo neutrons, the estimated floor-scattering component was well below 1%.

III. WELL-RESOLVED LEVELS

A. Energy Spectrum

In Fig. 3(a) is shown the pulse-height distribution at 0° for $E_\alpha = 7.96$ MeV and in Fig. 3(b) is shown the corresponding energy spectrum reduced to $\sigma(\theta,E)$, the neutron production cross section in laboratory coordinates. The three well-resolved levels corresponded to n_0, n_1, and n_2 neutron groups from the ^{9}Be$(\alpha,n)^{12}$C reaction, and were converted to $\sigma_0(\theta)$, $\sigma_1(\theta)$, and $\sigma_2(\theta)$ in the center-of-mass system.

B. n_0 Group

The variation of the cross section of n_0 neutrons with angle is shown in Fig. 4 for $E_\alpha = 6.79$, 7.96, 8.91, and 9.92 MeV. At the three highest energies a three-peaked

angular distribution is observed which does not change much with E_α. However, the angular distribution changes significantly between 7.96 and 6.79 MeV. At the lowest energy, it takes on a two-peaked shape that is very much like the fore-aft peaking reported by Gale and Garg[2] at $E_\alpha = 5.5$ to 6 MeV. At the three higher energies, the angular distributions are similar to those reported by Kjellman and Nilsson[3] for $E_\alpha = 10$ to 14 MeV and by Kondo et al.[4] for $E_\alpha = 17.5$ to 22 MeV. Thus, $\sigma_0(\theta)$ varies slowly with E_α between 8 and 22 MeV. Borrowing from the conclusions of Kjellman and Nilsson,[3] and of Calvert et al.,[15] the slow variation of the angular distribution with E_α indicates that direct reaction mechanisms dominate in the ^{9}Be$(\alpha,n_0)^{12}$C reaction for $E_\alpha > 8$ MeV. Although the angular distribution was found to be slowly varying from 7 MeV down through 5.5 MeV, it varies much more rapidly with
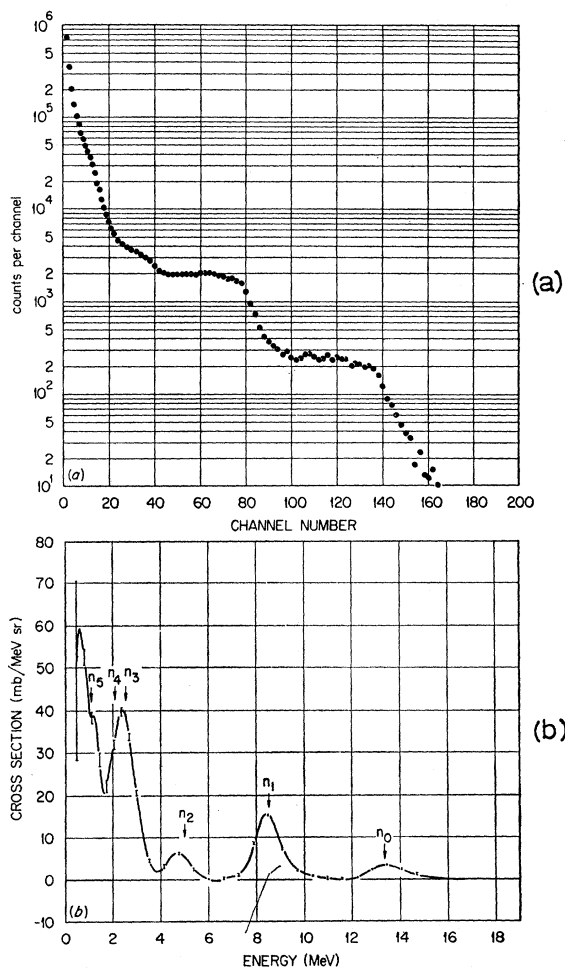

FIG. 3. Cross section for ^{9}Be(α,n) reactions (lab system) at 0° for $E_\alpha = 7.96$ MeV. The arrows show the energies of the neutron groups from ^{9}Be$(\alpha,n)^{12}$C, ^{12}C*, assuming narrow linewidth. Part (a) shows the raw data.

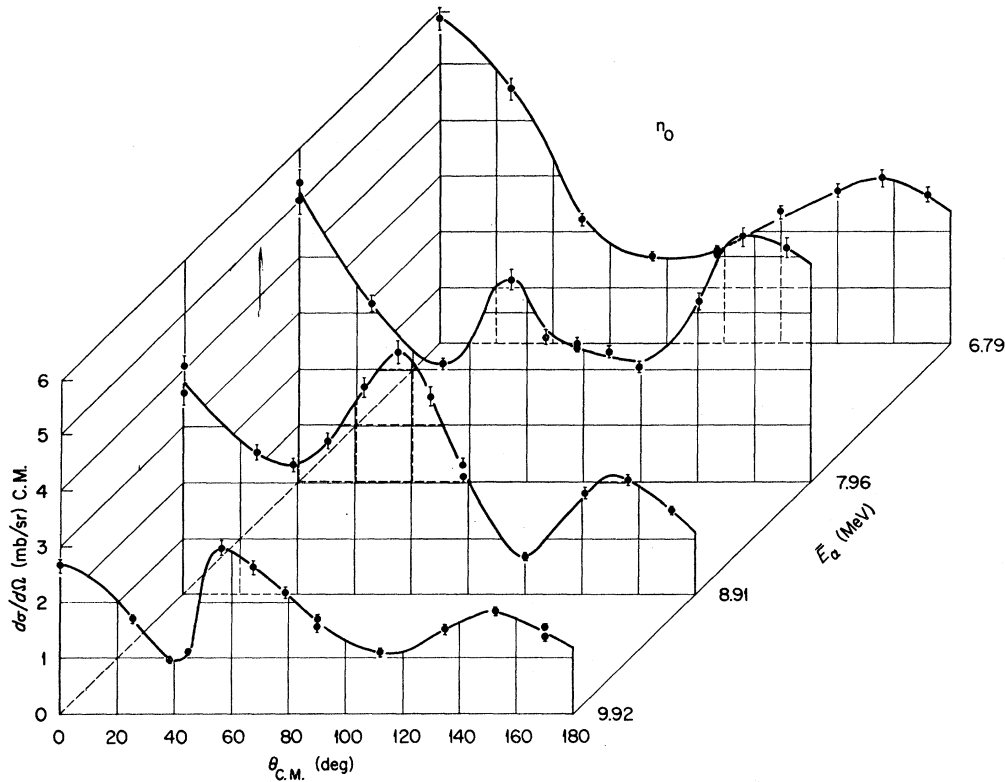[15] J. M. Calvert, N. H. Gale, J. B. Garg, and K. Ramavataram, Nucl. Phys. **31**, 471 (1962).

FIG. 4. Cross section (c.m.) versus angle of n_0 neutrons for four values of E_α.

E_α from 5.1 down to 2 MeV.[2,16] In fact, the data below 5.1 MeV are apparently accounted for only with compound nucleus theory.[16] This may not be inconsistent with the data on the highest-energy groups at higher E_α values, since compound nucleus reactions are expected to be strongest for the lower-energy neutrons.

In Fig. 5 is shown a fitting to the measurements with a plane-wave Born-approximation calculation in which roughly equal parts of knockout reaction and of the heavy-particle stripping of Owen and Madansky[17] are assumed. The fit is only fair, for reasons discussed in the

conclusions. In addition, it may be fortuitous because no reasonable fit could be made at the three energies above 6.79 MeV. These calculations were made with the equations given in Ref. 18.

Integration of $\sigma_0(\theta)$ over angle yielded σ_0 at the four values of E_α. The results presented in Table I show a

TABLE I. Total cross section for the well-separated neutron groups, n_0, n_1, and n_2. The total cross section for the inverse ^{12}C$(n,\alpha_0)^9$Be reaction and the corresponding neutron-bombarding energy are shown, as calculated from the ^{9}Be(α,n_0) cross section.[a]

E_α (lab) (MeV)	$\sigma(\alpha,n)$ (mb)			$\sigma(n,\alpha_0)$ (mb)	E_n (lab) (MeV)
	n_0	n_1	n_2		
6.79	30	138	31	81	11.3
7.96	36	113	24	103	12.1
8.91	30	66	19	93	12.8
9.92	22	74	13	72	13.6

[a] The reciprocity relation $\sigma(n,\alpha_0)(2I_1+1)M_\alpha E_\alpha = \sigma(\alpha,n_0)(2I_2+1)M_n E_n$ was used. $I_1 = 3/2$, $I_2 = 1/2$, M_α and M_n are reduced masses, and E_α, E_n are in the center-of-mass system.

[16] J. R. Risser, J. E. Price, and C. M. Class, Phys. Rev. **105**, 1288 (1957).

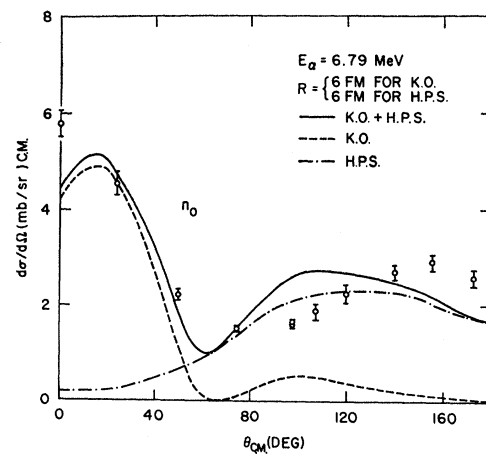[17] G. E. Owen and L. Madansky, Phys. Rev. **105**, 1766 (1957).

FIG. 5. A fit to the measured data with incoherent addition of roughly equal parts of knock-out and heavy-particle-stripping neutrons at $E_\alpha = 6.79$ MeV. Plane-wave Born-approximation calculations were utilized (see Ref. 18).

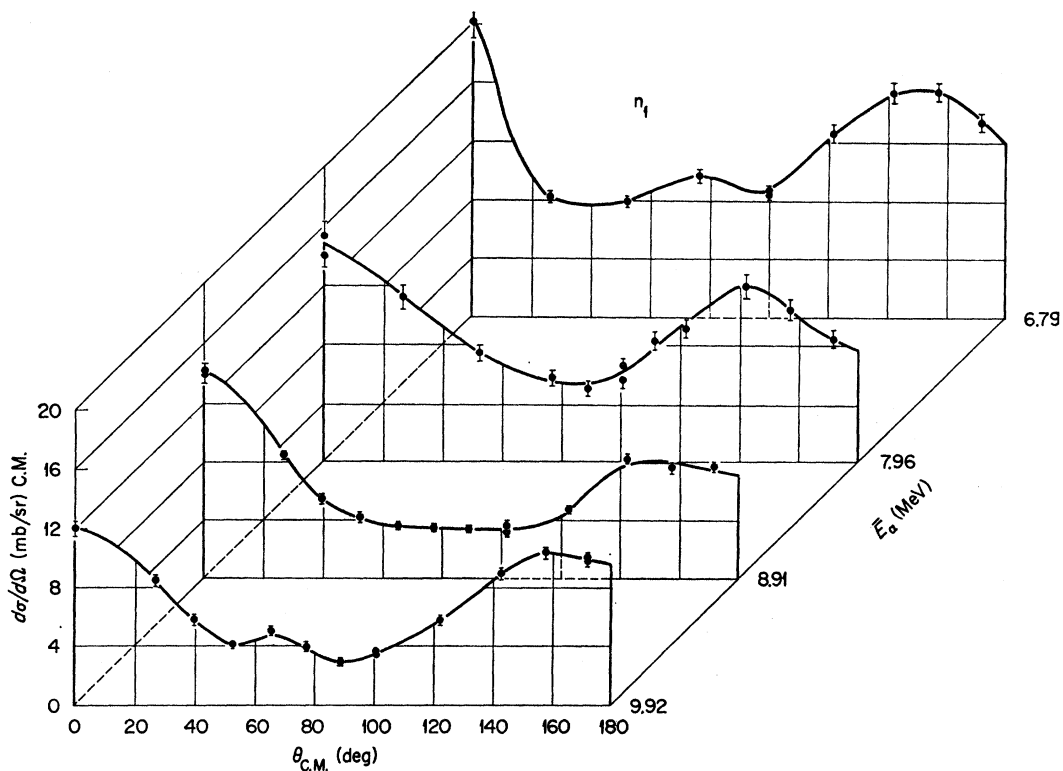[18] W. D. Ploughe, E. Bleuler, and D. J. Tendam, Phys. Rev. **124**, 818 (1961).

FIG. 6. Cross section (c.m.) versus angle of n_1 neutrons for four values of $\bar{E}_\alpha$.
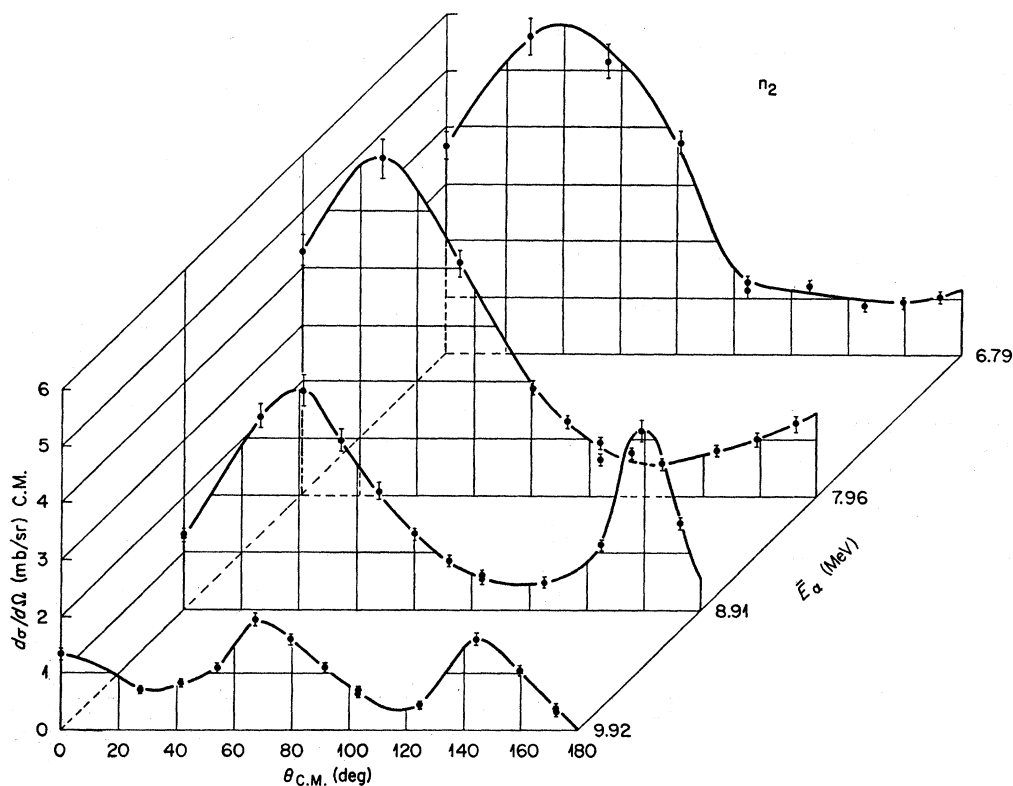

FIG. 7. Cross section (c.m.) versus angle of n_2 neutrons for four values of $\bar{E}_\alpha$.

peak at 8 MeV, then a gradual decrease to $E_\alpha = 10$ MeV. The value of $\sigma(\alpha,n_0)$ at 9.92 MeV is 22 ± 2 mb, and compares favorably with the value 24 ± 6 mb calculated from the observed cross section $\sigma(n,\alpha_0)=80\pm20$ mb (Ref. 19) for the inverse ground-state transition, $^{12}C(n,\alpha)^9Be$, at $E_n=14.1$ MeV. The agreement is very good and serves as an independent check on our systematic error. In addition, we calculated the cross sections of the $^{12}C(n,\alpha)^9Be$ ground-state transition for the four neutron-bombarding energies of 11.3, 12.1, 12.8, and 13.6 MeV corresponding to $E_\alpha=6.79$, 7.96, 8.91, and 9.92 MeV. (See Table I.)

C. n_1 Group

In Fig. 6 is shown $\sigma_1(\theta)$ for four values of E_α. The angular distributions display a persistent fore-aft peaking with a small third peak at the highest and lowest values of E_α. They are much like those reported by Kjellman and Nilsson[3] at 10 and 11 MeV, and somewhat similar to the fore-aft peaking reported by Gale and Garg[2] for E_α between 6 and 5.5 MeV, and by Risser et al.[16] for $E_\alpha=5.1$ down to 4 MeV. Thus, the variation of $\sigma_1(\theta)$ with E_α is quite slow between 4 and 11 MeV. The difference in shape between $\sigma_0(\theta)$ and $\sigma_1(\theta)$ must be related to the spins and parities (0+ and 2+, respectively) of the two corresponding levels for the ^{12}C residual nucleus, and possibly to a different nuclear configuration of the 0+ and 2+ states.

Attempts to fit the curves of Fig. 6 with knock-out and heavy-particle stripping reaction calculations showed very poor agreement at all four energies.

D. n_2 Group

The variation of $\sigma_2(\theta)$ with E_α, as seen in Fig. 7, is quite pronounced. At $E_\alpha=9.92$ MeV, three peaks can be seen. This changes to a two-peaked angular distribution at $E_\alpha=8.91$ MeV, and to a strong forward-

FIG. 9. Excitation functions for n_0, n_1, and n_2 neutrons at 0° (c.m. system) for $\bar{E}_\alpha=6$ to 10 MeV.
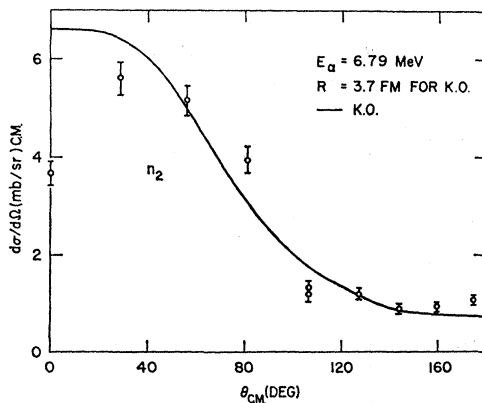

FIG. 8. A fit to the measured data with only the knock-out type of direct interaction assumed. A plane-wave Born-approximation calculation was utilized (see Ref. 18).

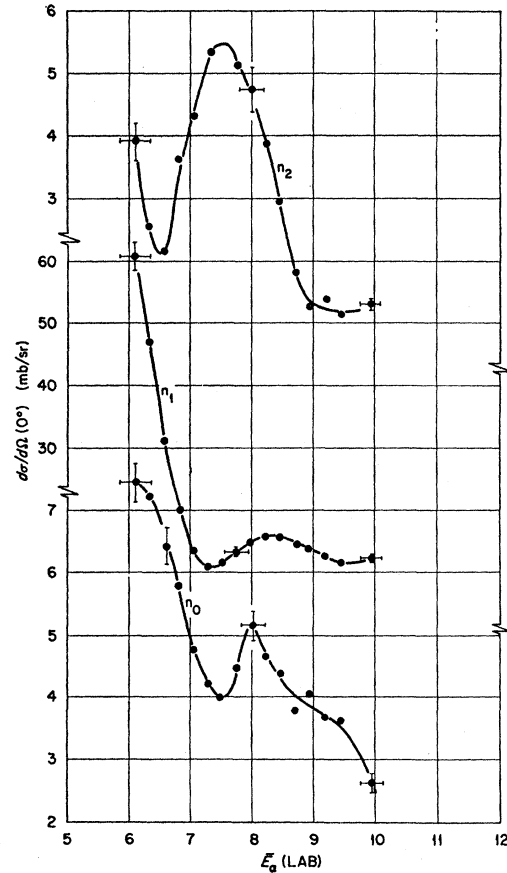[19] E. R. Graves and R. W. Davis, Phys. Rev. 97, 1205 (1955).

peaked shape at $E_\alpha=7.96$ and 6.79 MeV. At the lowest value of E_α, $\sigma_2(\theta)$ is very much like the three angular distributions for $E_\alpha=5.5$ to 6 MeV (Ref. 2), while for $E_\alpha=9.92$ MeV, the shape of $\sigma_2(\theta)$ is very much like that reported for $E_\alpha=9.8$ MeV (Ref. 3). Little variation of $\sigma_2(\theta)$ was observed for E_α between 10 and 14 MeV,[3] where $\sigma_2(\theta)$ looks very much like $\sigma_0(\theta)$. This similarity may be related to the fact that both final levels in ^{12}C have $J^\pi=0+$, and to the possibility that the two levels are otherwise quite similar.

Only the 6.79-MeV data showed some agreement with the Born-approximation calculations shown in Fig. 8. Only the knock-out mechanism was assumed. From this poor fit (see 0°) and from much poorer fits at higher energies, it appears that either the plane-wave calculations are too inaccurate, or that direct reaction mechanisms do not dominate. In any case, it is clear that no conclusions should be drawn until comparisons with careful distorted-wave Born-approximation calculations can be made.

E. 0° Excitation Functions

The 0° excitation functions are shown in Fig. 9 for the n_0, n_1, and n_2 neutron groups for $E_\alpha=6$ to 10 MeV.
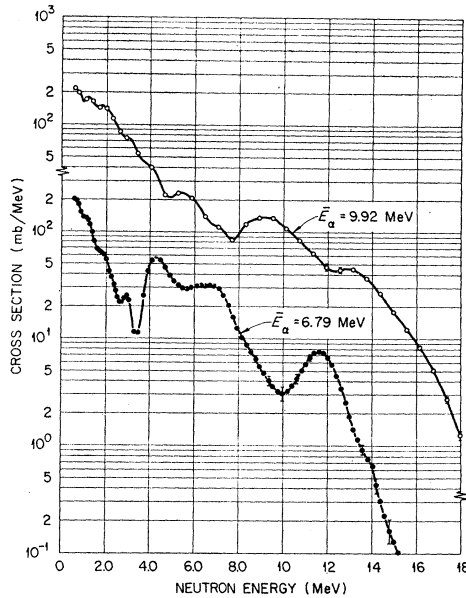
FIG. 10. Angle-integrated neutron cross sections versus neutron energy (lab system) for $\bar{E}_\alpha = 6.79$ and 9.92 MeV.

The n_0 excitation function is in reasonably good agreement with the high-resolution (in E_α) results of Miller and Kavanagh,[20] who used a stilbene crystal. However, our n_1 and n_2 curves are 50 to 80% higher; apparently the presence of the 4.43-MeV γ-ray pulses (which they used to obtain the 0° cross section for n_1 neutrons) that appeared below the highest n_0 neutron pulses in their data resulted in a substantial loss of accuracy. Our pulse-shape discriminator circuit was very effective in rejecting these γ-ray pulses.

While the 0° excitation functions are of interest as an independent check on our systematic error, they may be of limited value in showing resonance structure. A slight shift of the forward peak in the neutron angular distribution can result in a very large change of $\sigma(0°)$ without the presence of a corresponding change of $\sigma = \int_\theta \sigma(\theta)d\Omega$, the angle-integrated cross section.

IV. LOW-ENERGY DETAILS OF THE NEUTRON SPECTRA

A. Energy Spectrum at a Fixed Angle

In Fig. 3, the peaks below the n_2 peak ride on a low-energy continuum which is probably due to the very broad n_4 level under the n_3 peak and some low-energy neutrons from other low Q-value reactions. Similar structure was observed in careful time-of-flight work at $E_\alpha = 13.5$ and 13.9 MeV and was analyzed by Nilsson and Kjellman.[1] They were able to separate the n_3, n_4, and n_5 levels with the help of shape analysis of the broad n_4 level. At these values of E_α, the low-energy component from other reactions did not interfere with analysis of

[20] R. G. Miller and R. W. Kavanagh, Nucl. Phys. **88**, 492 (1955).

the n_3, n_4, and n_5 neutron groups, as it would at the values of E_α used in the present work. They found that the n_4 level interfered very slightly with the n_2 level, that it peaked at about the position of the sharper n_3 peak, and that it raised the very weak n_5 peak appreciably. Thus, in Fig. 3, it appears that the n_3 peak is raised mostly by the broad n_4 level. The n_5 peak is raised partly by the tail of the n_4 level, but mostly by low-energy neutrons from competing reactions, such as $^9\text{Be}(\alpha,\alpha')^9\text{Be}^* \rightarrow {}^8\text{Be} + n$, $^9\text{Be}(\alpha,{}^8\text{Be})$ $^5\text{He} \rightarrow {}^4\text{He} + n (\tau \sim 10^{21} \text{ sec})$, and $^9\text{Be}(\alpha,n)$ 3α, which have much smaller Q values than the $^9\text{Be}(\alpha,n)$ ^{12}C reaction.

B. Energy Spectrum Integrated Over Angle

The neutron-production cross section was numerically integrated over angle according to the prescription $\sigma(E_i) = \sum_j \sigma(\theta_j, E_i)\Delta\Omega$. The results for $E_\alpha = 6.79$ and 9.92 MeV are shown in Fig. 10. These spectra show much structure at high neutron energies, as expected, but also show an evaporation like component that hardens with increasing E_α. The hardening is indicated by the increase in "nuclear temperature" with E_α (see Table II), where the "temperature" was obtained from the slope of a plot of $\sigma(E_n)/(E_n\sigma_c)$ versus E_n (σ_c is the neutron-capture cross section of the excited final nucleus, as calculated from continuum theory[21]). This increase in slope implies that the low-energy neutrons must be due to lower Q-value reactions where three- and four-body breakup occurs, such as reactions mentioned in the preceding paragraph, because the level density of ^{12}C is low at these excitation energies. The three- and four-body breakup provides a larger number of degrees of freedom which would explain the presence of the steep slope (and its variation with E_α) at the low-energy region of the neutron spectrum.

C. Total Neutron-Production Cross Section

The integral of each neutron spectrum, such as those shown in Fig. 10, provides the total cross section for the production of neutrons above 0.5 MeV, our spectrometer cutoff. In Table II these totals are compared with

TABLE II. Total neutron-production cross section as measured with flat counter[a] compared with present results for $E_n > 0.5$ MeV. The hardness of the low-energy end of the spectrum is indicated by the reciprocal slope T obtained from a logarithmic plot of $\sigma(E)/\sigma_c E \cong \exp(-E/T)$.

E_α (MeV)	σ_t (mb)	σ_t above 0.5 MeV (mb)	Fraction of total >0.5 MeV	Reciprocal slope T (MeV)
6.79	570	390	0.69	0.52
7.96	660	466	0.71	0.57
8.91	755	535	0.71	0.68
9.92	703	518	0.74	0.95

[a] See Ref. 5.

[21] J. M. Blatt and V. F. Weisskopf, *Theoretical Nuclear Physics* (John Wiley & Sons, Inc., New York, 1952).

the flat-counter results of Gibbons and Macklin,[5] who used a 4π graphite integrating sphere to obtain σ(total) as a function of E_α. Above 0.5 MeV, we obtain about 70% of their total cross section. Our results are in agreement with theirs if we maintain roughly the same slope (see Fig. 10) and integrate the results down to 0-MeV neutron energy. The persistence of these steep slopes at very low neutron energies, for all four values of bombarding energy E_α, can be much more plausibly explained with breakup reactions than with the ^{9}Be$(\alpha,n)^{12}$C reaction. The above inferences assume that there are no systematic differences in absolute normalization of the present results and those of Gibbons and Macklin,[5] a reasonable assumption since both sets of measurements employed the same targets, Faraday cup, current integrator, Van de Graaff accelerator, and analyzing magnets.

V. SUMMARY AND CONCLUSIONS

From the present data, and those of Refs. 3 and 4, the angular distribution for the n_0 neutron group varies slowly with bombarding energy for E_α from 8 to 23 MeV. [This observation is at variance with the conclusion of Deconninck et al.,[22] who have measured $\sigma_0(\theta)$ and $\sigma_1(\theta)$ between 13 and 23 MeV. Although there are similarities between their angular distributions and those of Kondo et al.[4] for $E_\alpha = 17.5$ to 22 MeV and those of Kjellman and Nilsson[3] for $E_\alpha = 10$ to 14 MeV, it is not clear that there is substantial fluctuation in the n_0 angular distribution between 13 and 17 MeV.] The slow variation of the angular distribution is perhaps due to direct interactions, with very little interference from compound nucleus effects.

Evidence of appreciable contribution of direct interaction was reported in the ^{9}Be$(\alpha,n\gamma)^{12}$C angular correlation work of Garg et al.[23] In addition, the ^{11}B$(\alpha,n)^{14}$N work of Calvert et al.[15] shows that many of the angular distributions for $E_\alpha = 2.2$ to 5.4 MeV can be explained by a combination of direct plus heavy-particle stripping. Similar conclusions can be stated for the ^{13}C$(\alpha,n)^{16}$O measurements and analysis by Nilsson and Kjellman.[24]

Besides the slow variation of angular distribution with E_α, the present measurements gave some additional weak evidence of direct interactions by producing two angular distributions that could be fitted with plane-wave Born-approximation calculations. A fitting of only two angular distributions may not be surprising in view of the fact that the plane-wave Born-approximation calculation is probably too crude an approximation to the distorted-wave Born-approximation (DWBA) calculations (e.g., see Ref. 17). It would therefore be interesting to compare these results with DWBA calculations in which varying proportions of knock-out and heavy-particle stripping are used as fitting parameters, keeping in mind that some backward peaking can be obtained with DWBA calculations without assuming the heavy-particle stripping process.[25] Unfortunately, such calculations are not easy, and generally require such inputs as optical-potential parameters derived from both α-particle and neutron-elastic scattering.

The neutron spectra at low energies show a strong low-energy component in the forward hemisphere. Integration of these spectra over angle results in a spectrum $\sigma(E)$ with a low-energy component that behaves much like that expected for three- and four-body breakup reactions of relatively low Q value. Integrating this spectrum from the 0.5-MeV spectrometer cutoff to maximum neutron energy, and comparing the results with the total cross section measured with a 4π flat counter,[5] we find that the low-energy component contributes appreciably to the total ^{9}Be(α,n) yield. This finding is of interest in the shielding of space vehicles that may be exposed to solar-flare α particles,[26] since beryllium alloys are good candidates for construction of the skin material of such vehicles. In fact, this area of interest provided the initial motivation and the support of the present work.

ACKNOWLEDGMENTS

[22] G. Deconninck, M. de Vroey, J. B. Meulders, and J. Simonet, Nucl. Phys. 49, 424 (1963).

[23] J. B. Garg, J. M. Calvert, and N. H. Gale, Nucl. Phys. 19, 264 (1960).

[24] A. Nilsson and J. Kjellman, Arkiv Fysik 21, 551 (1962).

[25] T. B. Day, L. S. Rodberg, and J. Sucher, Phys. Rev. 123, 1051 (1961); W. Tobocman, ibid. 115, 98 (1959).

[26] P. S. Freier and W. R. Webber, J. Geophys. Res. 68, 1605 (1963).